IEEE Access
Multidisciplinary ⋮ Rapid Review ⋮ Open Access Journal

Received 21 November 2023, accepted 23 January 2024, date of publication 29 January 2024, date of current version 6 February 2024.

Digital Object Identifier 10.1109/ACCESS.2024.3359273

RESEARCH ARTICLE

Drone-Assisted Cooperative Routing Scheme for Seamless Connectivity in V2X Communication

OMER CHUGHTAI[1], (Member, IEEE), NADIA NAWAZ QADRI[1], (Senior Member, IEEE), ZEESHAN KALEEM[1,2], (Senior Member, IEEE), AND CHAU YUEN[3], (Fellow, IEEE)

[1]Department of Electrical and Computer Engineering, COMSATS University Islamabad, Wah Campus, Wah Cantt 47040, Pakistan
[2]Islamic University Centre for Scientific Research, The Islamic University, Najaf, Iraq
[3]School of Electrical and Electronics Engineering, Nanyang Technological University, Singapore 639798

Corresponding author: Zeeshan Kaleem (zeeshankaleem@gmail.com)

This work was supported in part by NTU Startup Grant 022990-00001, and in part by the National Research Program for Universities (NRPU), Higher Education Commission (HEC), Pakistan, under Project 15355.

ABSTRACT The Intelligent Transportation System (ITS) has the potential to significantly improve communication reliability, efficiency, and manageability in transportation systems. Vehicular ad hoc networks (VANETs) are particularly valuable for sustaining ITS features in dynamic, high-density environments. Integrating the Internet of Things (IoT) into modern transportation systems can further enhance ITS capabilities by providing real-time data and connectivity. Challenges like insufficient spectrum utilization and increased end-to-end latency in single-radio data transmission systems have led to the development of advanced techniques such as dual-radio multi-channel systems. However, these approaches often compromise network performance due to interference. To address these limitations, this paper proposes drone-assisted cooperative routing (DACR), incorporating IoT elements for improved connectivity and data exchange. Performance evaluation, based on comparative analysis with existing state-of-the-art schemes, indicates that the proposed DACR outperforms in packet delivery ratio, end-to-end delay, and control message overhead. DACR demonstrates a 22% and 52% reduction in control message overhead compared to U2RV and CRRA, a 23% improvement in ETE delay over U2RV, a 33% improvement over CRRA, and a 14.5% and 44% increase in PDR, respectively.

INDEX TERMS Cooperative routing, seamless connectivity, flying ad hoc network, vehicular ad hoc network, vehicle-to-everything (V2X) communication.

I. INTRODUCTION

Vehicular networks (VNs) empower vehicles by integrating various wireless communication technologies such as Wi-Fi (802.11p), Cellular Networks (5G and beyond), Dedicated Short-Range Communication (DSRC), and Internet of Things (IoT) into a cohesive network architecture. The incorporation of such technologies addresses the critical challenge posed by the rise in fatalities associated with increased automobile usage [1]. Recognizing this as a significant problem, one of the promising solutions is to establish ad hoc coordination among vehicles as they come into proximity, which is referred to as Vehicular Ad hoc Networks (VANETs). In the context of the Intelligent Transportation System (ITS), VANETs play a pivotal role in facilitating safe and efficient vehicle navigation.

The reliance on a shared medium and a single radio transceiver in VANETs becomes problematic with the growing number of vehicles, leading to increased collision risks and degraded network performance. Challenges like disconnectivity and slow data dissemination in dense VANETs contribute to more end-to-end (ETE) latency and reduced throughput. While dual-radio devices promise to optimize spectrum use, cross-channel interference within the same band remains a notable concern. Addressing these challenges is essential for enhancing VANET effectiveness within ITS. The evolution to Vehicle-to-Everything (V2X) signifies a paradigm shift from VANETs, extending communication beyond vehicle-to-vehicle (V2V) and vehicle-to-infrastructure (V2I) to include pedestrians (V2P), drones

The associate editor coordinating the review of this manuscript and approving it for publication was Arun Prakash.

Seamless connectivity of vehicles holds the potential to improve driving efficiency and safety since the vehicle can directly interact with other nodes, the infrastructure, the pedestrian, the drone, and the cloud, which is the **Vehicle-to-X (Vehicle-to-Everything)** communication.

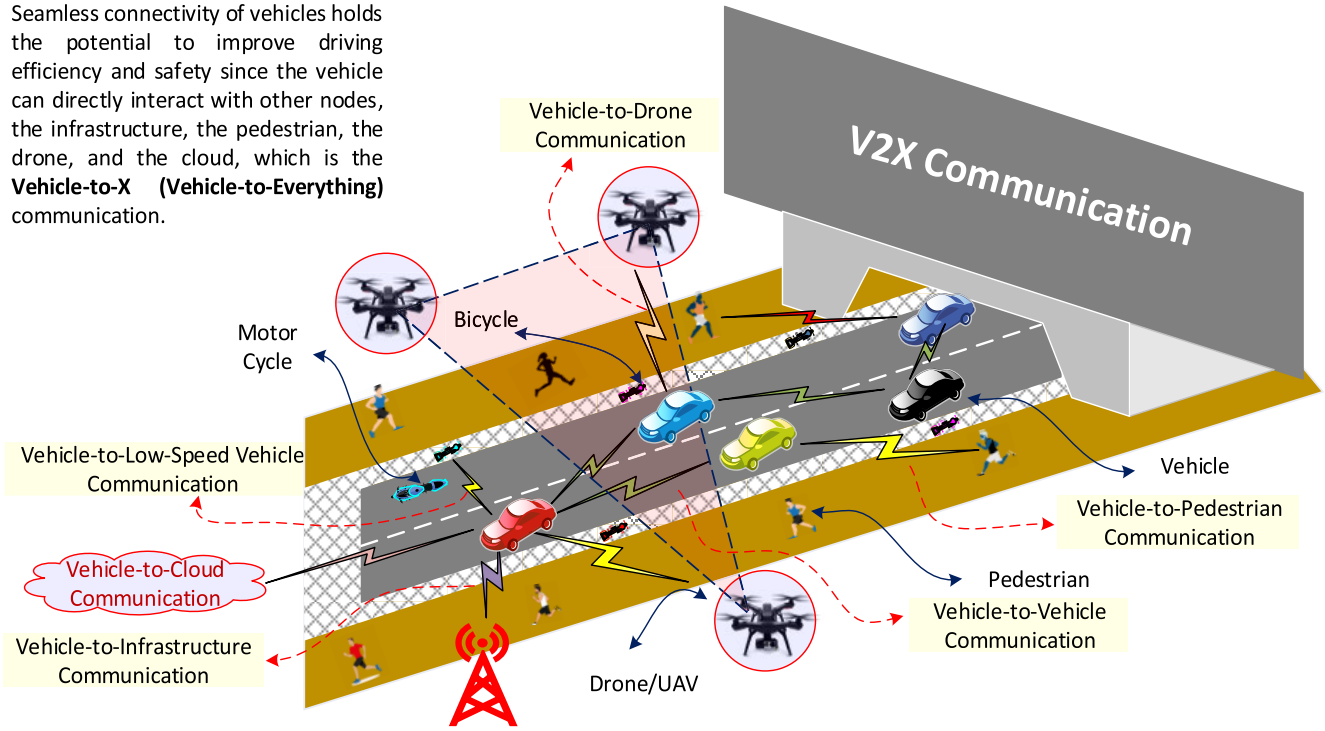

FIGURE 1. A unified vehicular environment with VANET connecting vehicles, infrastructure, pedestrians, drones, low-speed vehicles, and networks (V2X).

(V2D), networks (V2N), and more, as shown in Figure 1. This shift, driven by factors [2] such as diversification of communication, sensor integration, advanced connectivity standards, enhanced applications, and a holistic approach to ITS, aims to create a more interconnected, intelligent vehicular environment for safer, more efficient, and smarter transportation systems.

V2X communication is crucial for future self-sufficient cars, utilizing a heterogeneous system with various protocols for data fusion. While Cooperative Intelligent Transport Systems (C-ITS) currently lack models for single-use instances, intelligent transportation enhances C-ITS effectiveness and safety, leading to the development of applications with intelligent algorithms for accident reduction and support from unmanned aerial vehicles (UAVs) in various use cases like collision avoidance and highly autonomous driving. The evolving transportation system is shifting from technology-driven structures to a statistics-driven ITS driven by advancements in communication technologies [3].

To overcome those challenges, existing researchers adopted three communication methods for vehicles: a basic approach, an enhanced version of AODV known as the Community-based Reliable Routing Algorithm (CRRA) [4], and a contemporary UAV-assisted scheme named UAV-assisted Reactive Routing Protocol for VANETS (U2RV) [5]. However, these schemes still fall short of meeting performance requirements due to their inability to achieve low end-to-end (ETE) latency and other critical constraints. To overcome those challenges, the proposed Drone-Assisted Cooperative Routing (DACR) consistently outperforms the CRRA, demonstrating substantial improvements, including a 20% enhancement in critical aspects such as message efficiency, travel time of information, and successful message delivery rates. The analysis part shows that DACR is a significant choice for ITS to design a reliable V2X system.

The remainder of this paper is structured as follows: A background to V2X is presented in Section II, with the addition of a literature review of recent studies on routing and the effectiveness of V2X communication. Section III discusses the proposed routing scheme for drone-assisted VANETs. In addition to presenting the system model, that section also presents the composite routing metric to choose the best next-hop node on the path between the source and the destination. Section IV provides the simulation results and analysis, which confirm the efficacy of the approach. The paper concludes in Section V.

II. LITERATURE REVIEW

Drones, forming a Flying Ad Hoc Network (FANET), enhance broadband remote communication with better line-of-sight (LoS) connectivity, especially compared to ground vehicles [6]. Simulations confirm the feasibility of FANETs, showcasing their potential for widespread use in both military and civilian applications globally [7]. The integration of drones into Vehicular Networks (VNs) is explored in Drone-aided Vehicular Networks (DVNs) [8]. DVNs leverage UAV communication to enhance network coverage, data

efficiency, and service quality, acting as relays between ground and aerial nodes [9]. Despite these advancements, there is currently no standardized design for communication and networking with drone-assisted VNs [10]. A study to dynamically deploy the anchor points in Multi-Access Edge Computing (MEC) hosts and assign vehicular User equipment (UE) is presented in [11] for low latency connectivity, aiming to minimize network reconfiguration overhead. The multi-objective ILP optimization model, coupled with a heuristic algorithm, demonstrated satisfactory trade-offs between resource usage, UE latency, network overhead, and algorithm running time. Despite these positive outcomes, there is a need for further real-world validation and exploration of scalability issues in larger vehicular networks.

The UAV-assisted approach, U2RV, introduced in [12], focuses on urban road safety to manage network congestion, particularly in densely populated urban scenarios with intersections. Vehicular networks are highly dynamic, leading to frequent disconnections and data loss in areas with varying node densities. Researchers in [13] address this issue by proposing a Delay Tolerant Network (DTN), employing a message replication technique and asynchronous communication to enhance transmission in conditions with significant delays and disconnections. The researchers in [14] presented promising results in predicting outage phenomena and adapting power control in V2X communications using machine learning techniques; however, there is a need for further validation in diverse real-world scenarios and consideration of potential challenges in extending data collection to a collaborative swarm of vehicles within a vehicular network infrastructure.

In [15], a comprehensive V2X communication architecture, utilizing multi-technology processing, deep learning, and blockchain, has been demonstrated with 98% accuracy in predicting vehicle connectivity, showcasing its potential impact in addressing the growing demands of autonomous vehicles and aerial networks for higher data rates, low latency, and reliability in a cost-effective manner. However, the computation complexity is very high because of the use of several tools and technologies. V2X communication technologies, conducted in a real-life highway environment with rigorous testing parameters [16], revealed that Cellular-V2X (C-V2X) provides a longer range than the existing technologies. C-V2X service message transmission through intelligent relay vehicle selection is presented in [17] based on channel quality indicator (CQI) and reliable distance thresholds, resulting in reduced ETE delay and improved packet reception compared to existing algorithms.

In the context of VANETs disconnections, [18] discussed how a FANET can assist by utilizing UAVs as relays with adaptive mobility to quickly re-establish links. However, this approach struggles with small communication gaps. To tackle this, [19] proposed an approach by combining traffic density, connection, and distance criteria for routing patterns, but it lacks information on vehicle positions. Those limitations have been addressed in [20] to precisely determine vehicle locations through periodic transmission of "HELLO" messages, albeit at the cost of increased control message overhead.

Based on the literature, we concluded that UAVs present a clear advantage in vehicular communication scenarios. Unlike traditional ground-based vehicles, UAVs possess the ability to navigate around obstacles and cover varied terrains, allowing for consistent data relay even in challenging environments. Leveraging this capability, this research introduces a drone-assisted cooperative routing strategy, a novel approach designed to enhance the efficiency of routing mechanisms in V2X communication. We briefly outlined the contributions of this paper as follows:

- The best node is selected among several nodes based on the composite metric. The composite metric considers both the characteristics of the node and the link between the nodes.
- Only those nodes disseminate the broadcast messages, which are in the direction of the destination node; the rest of the nodes discard the message, which decreases the overhead of control messages. The E2E delay decreases because the best nodes are along the route towards the destination.
- Local recovery is initiated in case of disconnection or link failure to select the best predecessor node among the available nodes within the vicinity. Assistance is carried out whenever there is a scenario where the vehicle moves away from the selected route or there is no vehicle available along the route.

III. PROPOSED DRONE-ASSISTED COOPERATIVE ROUTING SCHEME

In this section, we discuss the integration of a traditional VANET with a FANET, presenting a network model. It outlines the selection criteria for a composite routing metric to determine the most efficient route. The proposed DACR, a two-stage algorithm using broadcast messages and cooperative route requests and responses, is explained with reference to a specific scenario, illustrating the established ETE route.

A. NETWORK MODEL

In the network model, the combination of traditional VANET and FANET has $\mathcal{N}$ wireless nodes. In order to assist the nodes in VANET, $\mathcal{V}$ nodes are required. In addition, the proposed model assumes that a collection of drones/UAVs, designated as $\mathcal{U}$ has been deployed in the air. Here, $\mathcal{U}$ and $\mathcal{V}$ are related by the relationship $(\mathcal{U} \cup \mathcal{V}) \subseteq \mathcal{N}$. Each node in the $\mathcal{N}$ network includes a built-in wireless transmitter, whether flying or ground-based, and is pre-programmed with a unique node identification. On a flat surface, it is assumed that all moving objects have similar attributes in terms of their ability to process information, sensing range, and memory. To avoid complexity, this research does not address path discovery amongst the $\mathcal{U}$ nodes; that is, the routing of nodes in $\mathcal{U}$ falls outside the scope of this work. Each node $\mathcal{N}$, however, does

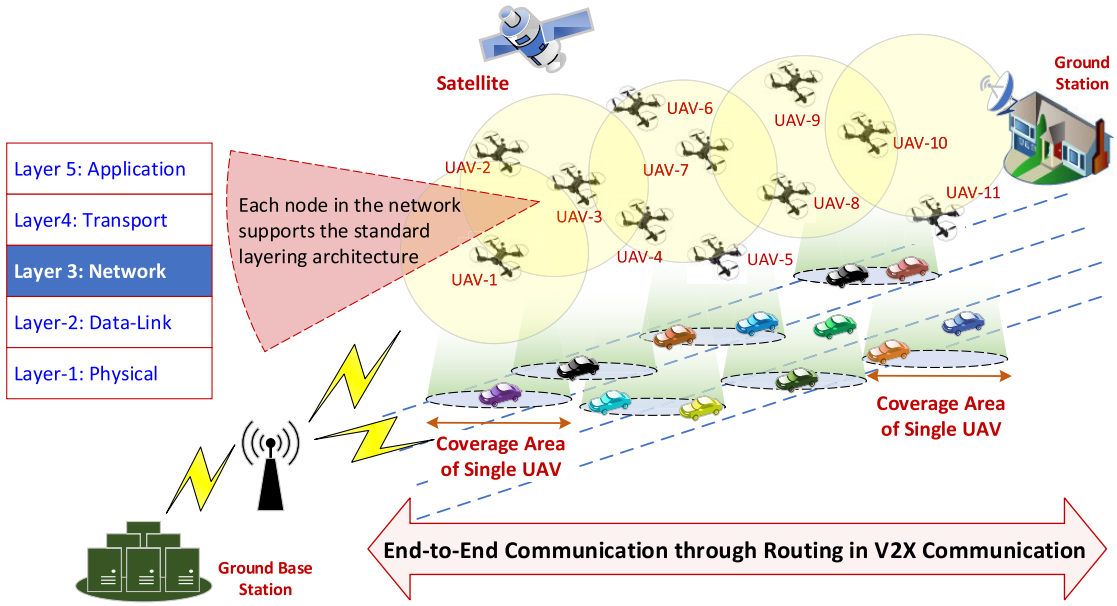

FIGURE 2. Drone-assisted cooperative routing scheme (DACR) system model to ensure connectivity during data communication.

include a GPS transceiver to track its location and has the capacity to update the routing tables.

Figure 2 depicts communication among the $\mathcal{V}$ nodes, which can get assistance from nodes $\mathcal{U}$ deployed in the FANET. In the scenario investigated, it is assumed that either congestion is presented as a result of high node density in a dense vehicular network environment or a communication gap has been formed during the course of data communication. It is to be noted that a ground station is capable of communicating with the UAVs and similarly, a ground base station is also available to communicate with the vehicles traveling along the roads and highways.

Whenever there is a route disconnection, UAVs $\mathcal{U}$ deployed in the overall network can serve as relay nodes for the $\mathcal{V}$ nodes, as discussed in [21]. In this relay mechanism, a source vehicle, denoted by $\mathcal{S}$, is permitted to start a communication session with a destination node, denoted by $\mathcal{D}$, in $\mathcal{V}$, such that $\mathcal{S}, \mathcal{D} \in \mathcal{V}$. Depending on which vehicle determines a disconnected zone, UAVs can receive messages from the ground station or from a vehicle that would not otherwise be able to access the channel, either because of congestion or because no other vehicle was within its vicinity, as shown in Figure 2. In either scenario, UAVs are requested to assist in bridging the gap between vehicles within disconnected zones.

A route discovery process presented in [22] adopted here for routing among the $\mathcal{U}$ drones to establish drone-assisted VANET. Assume that there are multiple routes $\mathcal{R}$ available in the network. Then the route between the selected $\mathcal{S}$ and $\mathcal{D}$ pair is represented as $\mathcal{R}_{\mathcal{SD}}$, and if there are multiple routes available between a pair of $\mathcal{S}$ and $\mathcal{D}$, then the representation is denoted by $\mathcal{R}^{\mathcal{K}}_{\mathcal{SD}}$. For r number of routes between a pair of $\mathcal{S}$ and $\mathcal{D}$, is represented as $\mathcal{R}_{\mathcal{SD}}{}^{1}, \mathcal{R}_{\mathcal{SD}}{}^{2}, \cdots \mathcal{R}_{\mathcal{SD}}{}^{r}$, such that $\mathcal{K} = 1, 2, 3, \cdots r$.

In DACR, each vehicle i in $\mathcal{V}$ determines front and rear or behind zones represented as FZn_i and BZn_i, respectively, with reference to its neighbors Nbr_i. Thus, $(FZn_i \cup BZn_i) \subseteq Nbr_i$ or FZn_i and $BZn_i \in Nbr_i$, in a particular time period.

Figure 3 illustrates the situation for node 5. The entries shown in this figure contain the set of all nodes within the broadcast range of node 5, broken down into backward and forward nodes. All nodes that are to the rear of node 5 and within its communication neighborhood (broadcast range) are denoted as BZn, where $n = 5$, and all vehicles that are available towards the front part of vehicle 5 and within its communication vicinity (broadcast range) are denoted as FZn_i. Furthermore, the Allied Node Table, ANT_i, stores the non-congested vehicles and nodes among the nodes accessible as FZn_i. The ANT nodes have the necessary capabilities to be a part of a reliable discovered route $\mathcal{R}^{\mathcal{K}}_{\mathcal{SD}}$. Among all the nodes in ANT, the best node or vehicle is chosen in accordance with the Composite Routing Metric (CRM). The procedure to determine the CMR and the procedure to discover a reliable and efficient route using a Cooperative Route Request (CRRQ) and Cooperative Route Response (CRRS) are discussed next.

B. CRITERIA TO SELECT NEXT HOP AND THE WORKING PRINCIPLE OF DACR

In the scenario depicted in Figure 3 to demonstrate the criteria to select the next hop node and the operation of the proposed DACR, ten distinct vehicles from the group of vehicles $\mathcal{V}$ are shown in a vehicular environment under the auspices of a FANET and are connected via wireless links. The big circle shows the transmission range for vehicle number 5. Its neighbors are vehicles 2, 3, 4, 6, 7, and 8, which are present in NBr_5. Out of all the vehicles present in NBr_5, it is expected

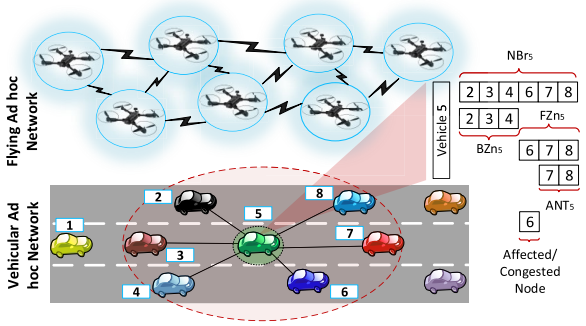

FIGURE 3. Broadcast range of node 5 with entries in NBr_5, BZn_5, FZn_5, and ANT_5.

that 2, 3, and 4 are in BZn_5. However, vehicles 6, 7, and 8 are in FZn_5. Vehicle 6 is likewise considered to be congested because it is transporting the maximum amount of traffic that a vehicle is permitted to carry.

1) DIRECTION TOWARDS DESTINATION

Every node in the network in this work is fully aware of the destination node and its location. The direction to a location can be simply predicted by this consideration. Additionally, procedures for separating the front and rear zones are developed. By taking into account the destination's direction and the relative speed of the neighbors, the nodes in the front zone of a particular node are selected. One advantage of taking into account the aforementioned criteria is reducing the number of nodes that generate broadcasts. The nodes that do not meet the routing criteria are those forming the rear or behind the zone of a given node. Consequently, they are not permitted to rebroadcast a message. As a result, there are fewer control messages sent throughout the network. The selection of the subsequent hop from the front zone is discussed as follows:

Nodes in the front zone are assumed to be the most suitable because they are either going in the direction of the destination or moving at a speed that is closer to the node where the decision to communicate is made. All of the nodes in the front zone that are congested or lack the resources necessary to handle the additional data flows are eliminated from routing consideration. Thus, a Cooperative Route Request (CRRQ) can only be rebroadcast by nodes that meet the requirements to be members of an ANT; otherwise, the receiving node must discard any such packet and is not permitted to take part in the routing process for a particular flow. The following representation is used to calculate the forwarding angle. It is also discussed in the authors' [22].

In Figure 4, taking N_0 to be the source node and N_4 to be the destination node, then N_1, N_2, and N_3 are intermediate nodes. The distances between nodes are indicated by solid lines for intermediate nodes. The distance from the destination to any particular node is indicated by a dotted line. A node is assumed to be in the front zone of a forwarding node of interest if the distance from that node to the destination is less than the distance from the forwarding node to the destination; otherwise, that node is in the behind zone (not present in this example, but see the later example).

Using the Euclidian distance formula, the distance between any specified node i and the destination is determined as follows:

$$D_i = \sqrt{(x_d - x_i)^2 + (y_d - y_i)^2}. \tag{1}$$

In (1), D_i is the distance of node i from the destination, (x_d, y_d) are coordinates of the destination node, while (x_i, y_i) are the coordinates of the node under consideration.

Then, based on (2), as discussed shortly, it can be computed that N_1 and N_2 lie in the front zone of the forwarding node N_0, in fact, the source node. Similarly in Figure 4, for forwarding or reference Node 2, N_3 and N_4 are in its front zone whereas N_1 is in its behind zone. Therefore, a route request generated by Node 2 will be discarded by Node 1 and will be rebroadcast by N_3 and N_4, as they are in the front zone of Node 2. In fact, as $N4$ is the destination node it will not rebroadcast in this example.

These BZn_2 and FZn_2 (or BZn_5 and FZn_5 in Figure 3) can be conveniently segregated using the forwarding angle given by (2). The symbol d_{rn_d} in (2) represents the distance between the reference or forwarding node and the destination node. The number d_{lh-rn} represents how far the previous forwarding node is from the reference or current forwarding node. d_{lh_d} indicates how far the previous forwarding node is from the destination. The forwarding angle is used to calculate and locate the nodes in both the front zone and the behind zone of any forwarding or reference node. Provided there is a less than or equal to the 180-degree angle between a particular forwarding or reference node (rn) and the last hop or previous forwarding node (lh), the target forwarding node is on a path in the direction of the intended destination (d), as it is in a forwarding zone.

$$\theta = cos^{-1} \frac{d_{rn\_d} - d_{lh-rn}}{\sqrt{\left(d_{lh\_d} - d_{lh-rn}\right)^2} - \sqrt{\left(d_{rn\_d} - d_{lh-rn}\right)^2}}, \tag{2}$$

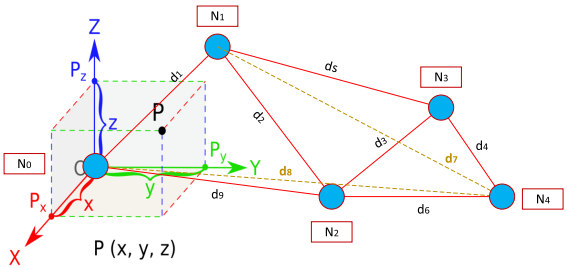

FIGURE 4. Forward angle calculation geometry using the last- or previous-hop forwarding node, the referenced or current forwarding node, and the destination node.

where $\theta \leq 180^o$. In (3), ξ_{max} stands for the maximum phase angle that a vehicle can have to be part of FZn_i and ξ_{θ_i} represents the phase angle of vehicle i. Then ξ represents the

normalized phase angle value of vehicle i and is represented as

$$\xi = \frac{\xi_{\theta_i}}{\xi_{\theta_{max}}}, \tag{3}$$

where, $\xi_{\theta_{max}} = 180^0$, and $60^0 \leq \xi_{\theta_i} \leq 180^0$. A function to represent the velocity of node i on the kth route toward the destination is represented as

$$\phi_{\xi,NBr_i}(k,\theta_i) = \begin{pmatrix} \xi_{\theta_i} \\ i \in FZn_i \backslash D \end{pmatrix}. \tag{4}$$

In (5), we mathematically modeled to select a vehicle with a phase angle relatively closer in its direction of travel towards the destination. Thus, in (5), Φ_{ξ,FZn_i} represents an objective function for identifying a node with a relative phase angle within the FZn_i of all the neighbors NBr_i of node i towards the destination as

$$\Phi_{\xi,FZn_i} = \min_{k=1,\ldots,n} \left(\phi_{\xi,NBr_i}(k,\theta_i)\right). \tag{5}$$

Furthermore, the equation (6) demonstrates the extraction of the index of such a node as

$$m^{\xi}_{FZn} = \underset{k=1,\ldots,n}{argmin} \left(\phi_{\xi,NBr_i}(k,\theta_i)\right). \tag{6}$$

2) SPEED OF VEHICLE/NODE

While choosing the next hop, the speed of a vehicle is also taken into consideration. The speed of each node in the front zone is calculated in relation to the speeds of the other nodes in the front zone. A node with a comparable relevant speed is permitted to be included in the source-to-destination route and is calculated by (7).

$$\mathcal{V}_i = \frac{\mathcal{V}_{lh} - \mathcal{V}_{rn}}{\mathcal{V}_{\max}}, \tag{7}$$

where $\mathcal{V}_i$ stands for the relative velocity of node i, $\mathcal{V}_{lh}$ for the forwarding node, $\mathcal{V}_{rn}$ for the next-hop, and $\mathcal{V}_{max}$ for the node's maximum speed in the region, which was taken to be 120 km/h in [23].

In (8), Γ represents the normalized value of velocity, and $\xi_{\mathcal{V}_i}$ represents the velocity of vehicle i. In addition, ξ_{max} stands for the maximum velocity that a vehicle can have on a road.

$$\Gamma = \frac{\xi_{\mathcal{V}_i}}{\xi_{\mathcal{V}_{max}}}, \tag{8}$$

where, $\xi_{\mathcal{V}_{max}} = 120$ km/hr, and $0 \leq \xi_{\mathcal{V}_i} \leq 120$. Equation (9) is a function to represent the velocity of node i on the k-th route and represented as $\phi_{\Gamma,NBr_i}(k,\mathcal{V}_i)$:

$$\phi_{\Gamma,NBr_i}(k,\mathcal{V}_i) = \begin{pmatrix} \xi_{\mathcal{V}_i} \\ i \in FZn_i \backslash D \end{pmatrix}. \tag{9}$$

In (10), the procedure to select a vehicle by means of its relative speed is mathematically written as:

$$\Phi_{\Gamma,FZn_i} = \min_{k=1,\ldots,n} \left(\phi_{\Gamma,NBr_i}(k,\mathcal{V}_i)\right), \tag{10}$$

where, Φ_{Γ,FZn_i} represents an objective function to identify a node with the relative velocity within the FZn_i of all the neighbors NBr_i of node i. Finally, using (11) the index of such a vehicle is identified.

$$m^{\Gamma}_{FZn} = \underset{k=1,\ldots,n}{argmin} \left(\phi_{\Gamma,NBr_i}(k,\mathcal{V}_i)\right). \tag{11}$$

3) TRAFFIC LOAD

The traffic flows that pass via each node in the network are monitored. By establishing a path using the flooding ID, the source ID, and the broadcast IDs, these flows are identified. Congested nodes are ones that try to handle more flows than their maximum capacity; hence they are more prone to drop packets. As a working hypothesis, it has been assumed that globally an intermediate node can only hold seven flows at once.

In (12), ζ represents the normalized value of congestion level, and $\zeta_{f,i}$ represents the level of congestion based on the number of flows f entering and leaving a vehicle i. In addition, ζ_{max} stands for the maximum number of flows that a specific vehicle may support. Considering the example illustrated in Figure 3, node 5 has 3 flows entering it and two flows leaving it, as node 6 is found to be congested.

$$\zeta = \frac{\zeta_{f,i}}{\zeta_{max}}, \tag{12}$$

Here, ζ_{max} is assumed as 5, such that $0 \leq \zeta_{f,i} \leq 5$. The level of congestion at the k-th node carrying a flow f in (13) is calculated as:

$$\phi_{\zeta,NBr_i}(k,f) = \begin{pmatrix} \zeta_{f,i} \\ i \in FZn_i \backslash D \end{pmatrix}. \tag{13}$$

Using (14), we selected a vehicle with the least congestion and represented as

$$\Phi_{\zeta,FZn_i} = \min_{k=1,\ldots,n} \left(\phi_{\zeta,NBr_i}(k,f)\right), \tag{14}$$

where Φ_{ζ,FZn_i} represents an objective function to identify a node with the lowest level of congestion within the FZn_i of all the neighbors NBr_i of node i. In (15), among the nodes in FZn_i, m^{ζ}_{FZn} represents the index of the node with the lowest congestion level as

$$m^{\zeta}_{FZn} = \underset{k=1,\ldots,n}{argmin} \left(\phi_{\zeta,NBr_i}(k,f)\right). \tag{15}$$

Vehicles that are below the threshold for traffic congestion and are still present in the front zone (FZn) are kept in the ANT. For example, in Fig 3, vehicles 7 and 8 are members of the ANT, the best vehicle amongst them is selected using equation (15), and this selection is then used to calculate the composite routing metric during CRRS.

4) COMPOSITE ROUTING METRIC

The three criteria that make up a composite routing metric are direction toward the destination, relative speed, and congestion level. The best node from the list of ANT nodes that are currently accessible is selected using this Composite

Routing Metric (CRM). A CRM is used to select the best node among various candidates for each hop from the destination to the source during Cooperative Route Response (CRRS). However, the Cooperative Route Request (CRRQ) message will not be distributed in the network if its Time-to-Live (TTL) value is equal to 32 hops. This mechanism is also used in the CRRA protocol [4], [5] as part of the comparison in Section IV. The CRM is calculated using the weighted sum of direction, relative speed, and congestion level as

$$\text{CM} = \alpha \times m_{FZn}^{\xi} + \beta \times m_{FZn}^{\Gamma} + \gamma \times m_{FZn}^{\zeta}. \quad (16)$$

In experiments, equal weights are considered for all three criteria by setting α, β, and γ appropriately in (16), though other weightings can obviously be considered.

C. WORKING PRINCIPLE OF THE PROPOSED DACR

The working principle of the proposed DACR is elucidated through the scenarios presented in Figure 5(a) to Figure 5(d). In the vehicular network, nodes initially broadcast 1-Hop Hello messages to establish front and back zones, sharing data such as node position, traffic flow details, relative speed, and forwarding angle as shown in Figure 5(b) and elaborated in Figure 4. A broadcast message with a Cooperative Route Request (CRRQ) is initiated in the VANET and received by nodes with entries of the sending nodes in their Active Node Table (ANT) as referred to in Figure 5(c). The destination responds with a Cooperative Route Response (CRRS) upon receiving the CRRQ as shown in Figure 5(d).

ANT updates states periodically, and nodes utilize a composite routing metric (CRM) to determine the best route based on factors like signal strength. Data packets are then transmitted along the discovered best route, with local recovery initiated in case of disconnection or link failure, as shown in Figure 6. If local recovery proves unsuccessful, FANET is contacted for assistance, enabling data transmission through aerial nodes until it reaches the intended destination.

D. ASSISTANCE OF FANET

When one vehicle requires assistance from another during data exchange and local recovery fails to maintain the connection, such as when a link fails due to high congestion or when no other vehicle is available to assist (i.e., if it detects congestion or a gap), that vehicle must seek the nodes in another network for assistance. This is accomplished through a FANET, in which each node (drone or UAV) covers a larger area than the node in the VANET, as depicted in Figure 6. The FANET is selected as it has the additional advantage of improved coverage, which could well lead to a drop in latency resulting from fewer hops. The protocol to connect the vehicle with the UAV is the same as used in [24], where UAVs can also be equipped with DSRC modems to broadcast and receive data from DSRC-equipped aerial and ground vehicles. Note that UAVs are anticipated to fly at low altitudes so that, by flying closer to the ground, collisions with other aircraft can be avoided.

TABLE 1. Simulation parameters.

Parameters	Values
Frequency	2.4 GHz
Carrier Sense Threshold (CS_Thresh_)	5.01E-12
Receiver Threshold (RX_Thresh_)	3.65E-10
DataRate_	11 Mb
BasicRate_	1 Mb
Channel type	Wireless channel
Propagation model	Two-ray ground (VANET) Free space propagation (FANET)
Network interface type	Wireless phy
MAC type	IEEE 802.11p
Interface queue type	DropTail
Link layer type	LL
Antenna model	Omni antenna
Max. packets in queue	50
Number of nodes	Variable
Routing protocol	U2RV, CRRA, and DACR
Number of sources	Variable

IV. SIMULATION RESULTS AND DISCUSSIONS

This section presents a thorough simulation of the proposed DACR. Moreover, in Table 1, we summarized the key simulation parameters. Based on varying (i) packet inter-arrival time, (ii) number of nodes, and (iii) number of sources, the performance of DACR in comparison to U2RV [12] and CRRA [4] is assessed. The scenarios discussed above have been simulated using the network simulator (ns-2). It has a mechanism that allows for the implementation of different radio models, traffic models, and topologies. Another open-source simulator for simulating urban mobility is Simulation of Urban MObility (SUMO), which is patched into ns-2.31. It can easily generate traffic maps that include roadways, buildings, and edges, thus enabling the simulation of interactions involving vehicles, roadside units (RSUs), pedestrians, and aerial vehicles. When handling larger networks, it can generate various traffic patterns and topological configurations.

Mobility model generator for VEhicular networks (MOVE), which offers a geological modeling and analytical toolbox to analyze and integrate data, is also utilized in ns-2. It performs data analysis in both 2D and 3D environments. MOVE provides SUMO with vehicle movement capabilities for the simulation scenarios used in VANET. In ns-2.31, a number of parameters are taken into account in order to illustrate an urban mobility scenario.

Instantaneous throughput in vehicular networks with and without taking into account the aid of UAVs has been observed in drone-assisted IoT-enabled cooperative routing for seamless connectivity in V2X communication. In this scenario, the connected vehicle moved away, and data transmission was interrupted at a simulation time of 13 seconds, according to the analysis depicted in Figure 7. In spite of the vehicle's attempts to connect with any other vehicle to resume communication in an IoT-enabled network, in this case, there was not another vehicle nearby. As a result, the throughput is null. Contrarily, depending on cooperation, a vehicle has the capacity to link with the drone and continue the data transmission without any issues. The data keeps forwarding in this manner in the direction it is intended to go.

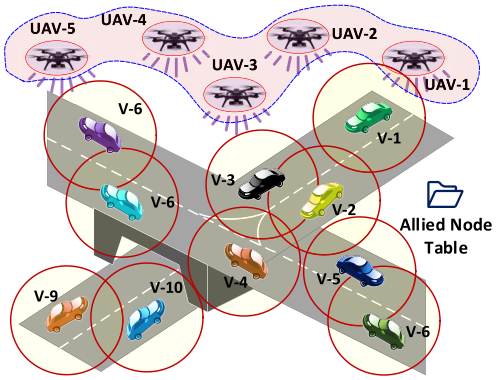

(a) Periodic broadcast of the HELLO messages

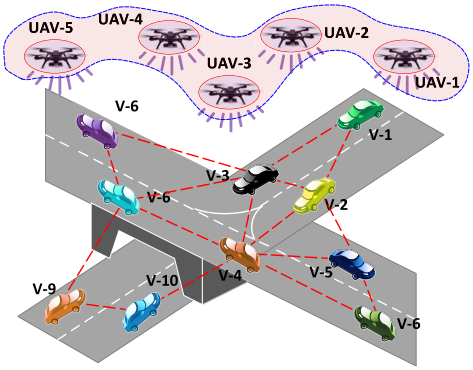

(b) Procedure for disseminating cooperative route requests

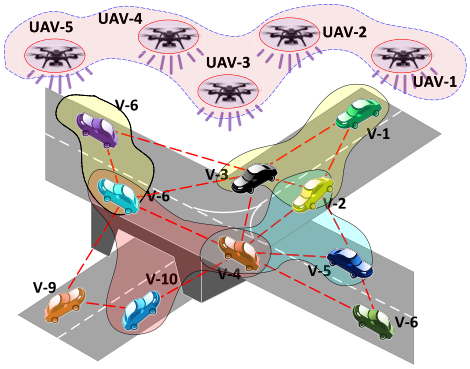

(c) Procedure for disseminating cooperative route response

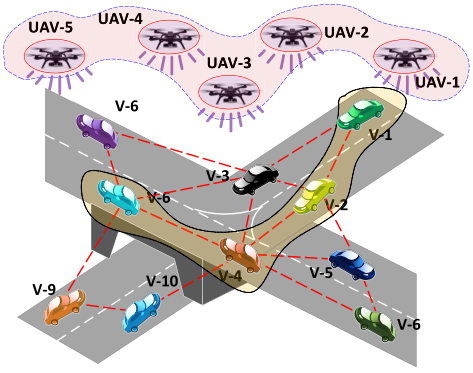

(d) End-to-End Cooperative Route Found/Discovered

FIGURE 5. A scenario depicting the working principle of DACR.

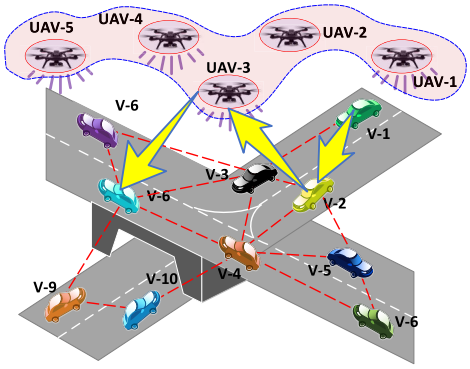

FIGURE 6. Getting assistance from UAVs during data communication.

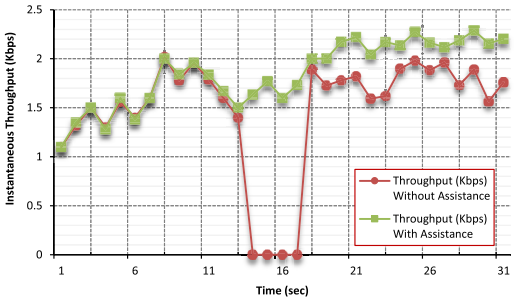

FIGURE 7. Impact of instantaneous throughput with and without assistance from a node in another network.

This demonstrates unambiguously that, in a case where there is no vehicular network node, support from another network improves performance in comparison to performance without assistance.

A. IMPACT OF VARYING PACKET INTER-ARRIVAL TIME

Figure 8 depicts the relationship between the ETE delay and packet inter-arrival time. It can be observed that the

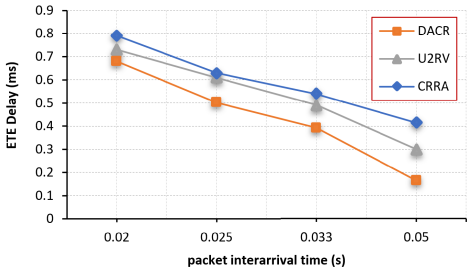

FIGURE 8. Impact of varying packet inter-arrival time on the ETE delay in a drone-assisted VANET consisting of 5 sources and 50 nodes.

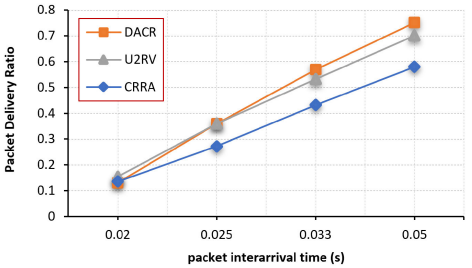

FIGURE 9. Impact of varying packet inter-arrival time on the packet delivery ratio in a drone-assisted VANET with 5 sources and 50 nodes.

rate at which packets are generated increases as the packet inter-arrival time decreases, causing the nodes along the ETE route to face substantial processing and queueing delays. As a result, the route discovery process must choose the next hop nodes based on the characteristics of the vehicles. The same phenomenon underlies DACR, which takes into account the signal quality and the characteristics of the vehicles to be selected in the discovered route.

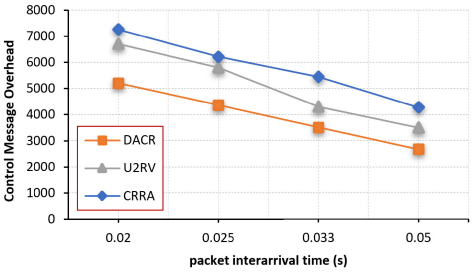

FIGURE 10. Impact of varying packet inter-arrival time on the control message overhead in a drone-assisted VANET with 5 sources and 50 nodes.

Additionally, the intermediate nodes in DACR have the ability to choose the subsequent hop during CRRQ using the CM routing criterion. Contrary to DACR, U2RV, and CRRA choose the forward vehicle based on a greedy approach. Because of this, the intermediate nodes are unable to choose the best next-hop node from their immediate neighborhood. As a result, the ETE delay is higher in U2RV and CRRA as compared to DACR. From the results in Fig 8, it can be observed that the ETE delay in the case of DACR is 23% less as compared to U2RV.

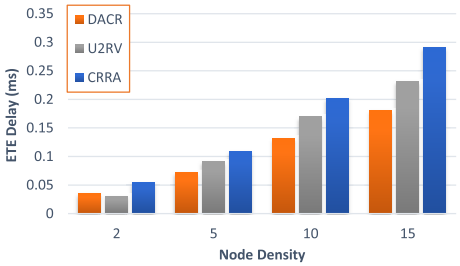

FIGURE 11. Effect of node density on ETE Delay with 100 nodes and 7 distinct numbers of sources.

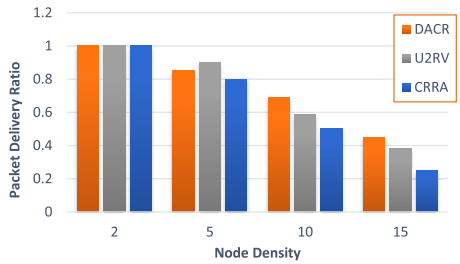

FIGURE 12. The impact of node density on packet delivery ratio is demonstrated using 100 nodes and seven sources.

Figure 9 depicts the effects of varied packet inter-arrival times on PDR with five distinct network sources. It is noticeable that a high traffic load of 50 packets per second results in a large number of lost packets. Because of this, the PDRs for DACR, U2RV, and CRRA are reduced. Less traffic generated by the sources decreases network congestion and decreases the packet loss ratio, which raises the Packet Delivery Ratio. In general, DACR outperforms U2RV and CRRA. This is a result of DACR selecting the best node with the least amount of traffic and choosing nodes that were heading in the direction of the destination.

Figure 10 shows the overhead of control messages in relation to the time between packet arrivals. Here, it is noticeable that DACR's control message overhead is significantly lower than that of the two other protocols. This is due to the fact that all network nodes use the front zone and forwarding angle to determine the Allied Node Table during neighbor discovery. As a result, fewer control messages are produced in DACR throughout the route discovery process. U2RV and CRRA, on the other hand, have a relatively high number of control messages. This is due to the fact that in U2RV and CRRA, as mentioned earlier, all nodes use greedy approaches and do not consider the characteristics of the vehicles moving toward the destination. As a result, it has been found that DACR has a 22% lower control message overhead than U2RV.

B. IMPACT OF VARYING NODE DENSITY

The node density of a network is the average number of a node's neighbors. With greater node density, the channel acquisition time to send the traffic grows. The time it takes to forward data packets is extended as a result. Figure 11

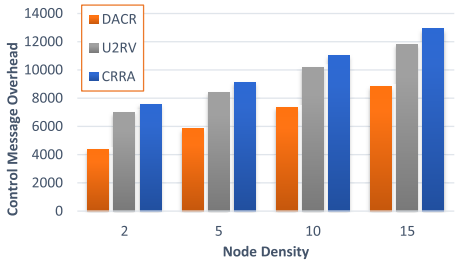

FIGURE 13. Impact of node density on control message overhead with 100 nodes and with 7 different sources.

compares the ETE latency to an increase in node density. The ETE delay was found to decrease across all protocols with a decrease in the number of neighboring nodes. However, DACR exhibits a 16% lower ETE delay than U2RV when an increase in node density occurs. This can be attributed to the fact that only allied nodes in the front zone are permitted to enter the channel in DACR, giving those nodes a high chance of acquiring the channel for data packets. As opposed to this, U2RV and CRRA reduce the likelihood of channel acquisition for data packets by requiring all neighboring nodes to acquire the channel for route discovery messages.

With a greater node density in the network, as shown in Fig 12, the PDR declines due to greater packet dropping. In a network with 100 nodes and a 2-node density, the PDR is 100% in the experiments. The PDR does, however, drop off as node density rises. Due to the selection of uncongested, near-destination nodes, DACR's drop rate is less than that of both U2RV and CRRA. U2RV exhibits a greater PDR decrease in contrast to DACR. This is because increased node densities lead to congestion on the nodes, which lowers the PDR in the network by increasing packet loss. Additionally, as node density increases, U2RV's overhead for control messages does as well. Additionally, U2RV and CRRA experience an increase in control message overhead when node density increases. Thus, according to Fig 13, DACR has a 31% lower control message overhead than U2RV in these circumstances.

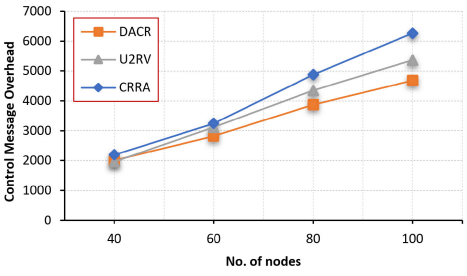

FIGURE 14. Impact of number of nodes on control message overhead with 6 sources packet inter-arrival time of 0.033swith simulation time of 100 s.

C. IMPACT OF VARYING NUMBER OF NODES

The control message overhead was also evaluated by varying the number of nodes in the network, as shown in Fig 14. DACR and U2RV exhibit an increasing trend in control message overhead according to the number of nodes. Nevertheless, DACR outperforms U2RV in terms of control message overhead. This can be attributed to the fact that a route found by DACR contains reliable nodes that are moving in the same direction as that of the destination and have a similar relative speed among the nodes in the path to the destination. Therefore, the chances of packet loss are reduced, and therefore, because of the stable route, the route request messages generated in the network are less.

Owing to this, the control messages overhead decreases. On the other hand, U2RV generates a high control message overhead with an increase in the number of nodes. This is because all the nodes in the network are required to disseminate the control messages needed to discover the destination, which in turn increases the number of route request messages and, hence, increases the control message overhead. Therefore, the control message overhead in DACR is 7% less than in U2RV.

Figure 15 shows the Packet Delivery Ratio of DACR and U2RV. It can be seen that with an increase in the number of nodes during a simulation time of 100 s and a packet inter-arrival time of 0.033 s for six different sources in the network, there is an increasing trend. However, because of the front zone and behind zone mechanisms used in DACR, more packets are received at the destination as compared to U2RV. Therefore, the PDR in DACR is 14.5% better than U2RV.

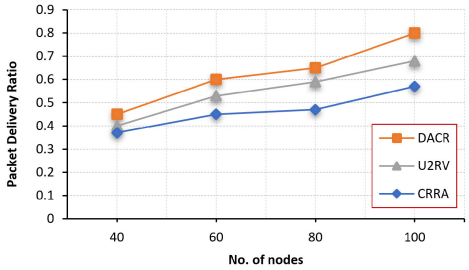

FIGURE 15. Impact of number of nodes on packet delivery ratio with 6 sources and packet inter-arrival time of 0.033swith simulation time of 100 s.

Usually, an increase in the number of nodes increases the ETE delay, as can be observed Fig 16. However, it has been observed that the ETE Ddelay is almost the same across the protocols under test, with 60 nodes in the network. However, with an increase in the number of nodes, the ETE delay in DACR is considerably less as compared to U2RV. This arises from the forwarding angle used to select the nodes that are heading towards the destination and are also reliable, as there is less congestion. In fact, the ETE delay in DACR is 14% less as compared to U2RV.

D. IMPACT OF VARYING THE NUMBER OF SOURCES

An analysis has been performed on how different performance metrics are impacted by the number of sources. Figure 17 depicts how control message overhead behaves

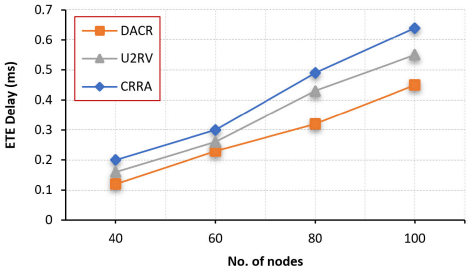

FIGURE 16. Impact of number of nodes on ETE delay with 6 sources and packet inter-arrival time of 0.033s with a simulation time of 100 s.

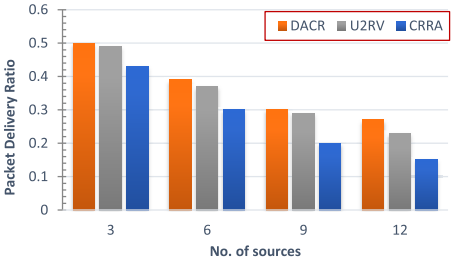

FIGURE 18. Impact of number of sources on packet delivery ratio using 40 nodes in the network with packet inter-arrival time as 0.02 s.

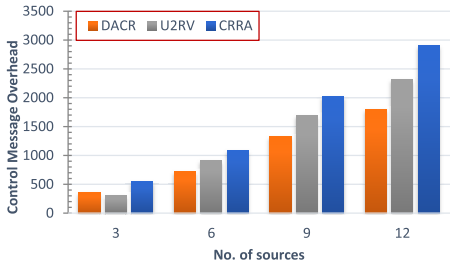

FIGURE 17. Impact of the number of sources on control message overhead with variable sources with packet inter-arrival time as 50 packets/s (0.02 s/packet).

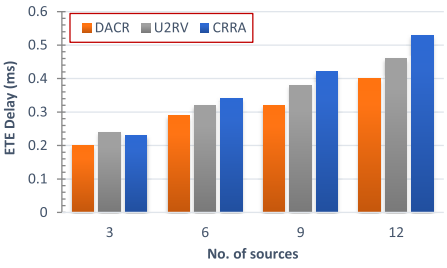

FIGURE 19. Impact of number of sources on ETE Delay with variable sources using 40 nodes in the network with packet inter-arrival time as 0.02s.

in relation to the number of network sources. Subject to a fixed number of network nodes, the overhead of the control message grows as the number of sources increases. This is because the increase in the number of sources increases the amount of traffic in the network, which increases the probability of congestion. This leads to an increase in packet loss, and hence, the nodes need to re-discover the route, which increases the control message overhead. However, in DACR, only the nodes in the front zone are allowed to broadcast the Cooperative Route Request messages. Therefore, the control message overhead is less in DACR as compared to U2RV. Quantitatively, DACR has 12.5% less control message overhead than U2RV.

Figure 18 shows the behavior of PDR according to the number of sources in the network. With an increase in the number of sources, the PDR decreases, subject to a fixed number of nodes in the network. This is because an increase in the number of sources increases the amount of traffic in the network, which increases the probability of congestion. This in turn leads to an increase in packet loss and, hence, the PDR decreases. This decrease is higher in CRRA, however, with a greater number of sources, U2RV shows competitive performance with respect to DACR. This is because it creates and maintains multiple paths. If one of the paths fails, it forwards the traffic to an alternate path, which increases the PDR in the case of U2RV.

Conversely, intermediate nodes (IMNs) could be part of numerous routes for various sources. As a result, all of the flows that IMN can handle could constitute a bottleneck. As a result, IMNs that are part of many routes may experience congestion. As a consequence, packet loss increases, which also causes the ETE delay to increase. According to Fig 19, this increase in U2RV is greater than in DACR. The route discovery process utilized in DACR is what accounts for the protocol's overall reduction in ETE time when compared to competing protocols. Overall, according to the simulation research, DACR showed a 7% lower ETE delay than U2RV.

V. CONCLUSION

One of the essential aspects of VANET that helps a network perform more efficaciously is the seamless dissemination of data traffic through efficient routing. However, in the highly dynamic environment of a VANET, disseminating messages to the intended destination without interruption, whether there is congestion due to high node density or when there is no next hop node available, is a challenging task. In this regard, a drone-assisted cooperative routing strategy (DACR) was proposed herein as a solution to this problem, whereby FANET helps VANET. A performance evaluation was carried out using the ns-2.31 network simulator and comparing DACR to U2RV, a state-of-the-art FANET-assisted VANET, and CRRA, a baseline routing protocol as a point of reference. The analysis of the results revealed that in the majority of scenarios, when considering PDR, ETE delay, and control message overhead, in comparison to U2RV and CRRA, DACR had reduced control message overhead by 22% and 52%, respectively. A 23% improvement in ETE Delay over

U2RV and a 33% improvement over CRRA have also been attained by DACR. Last but not least, compared to U2RV and CRRA, respectively, PDR has increased by 14.5% and 44%. Thus, DACR is a further step forward in FANET-assisted VANETs, pointing out the advantages of this line of research for the future concerning ITS.

REFERENCES

[1] S. A. H. Tabatabaei, M. Fleury, N. N. Qadri, and M. Ghanbari, "Improving propagation modeling in urban environments for vehicular ad hoc networks," *IEEE Trans. Intell. Transp. Syst.*, vol. 12, no. 3, pp. 705–716, Sep. 2011.

[2] G. Kumar and S. Mikkili, "Critical review of vehicle-to-everything (V2X) topologies: Communication, power flow characteristics, challenges, and opportunities," *CPSS Trans. Power Electron. Appl.*, early access, Oct. 13, 2023, doi: 10.24295/CPSSTPEA.2023.00042.

[3] J. Zhang and K. B. Letaief, "Mobile edge intelligence and computing for the Internet of Vehicles," *Proc. IEEE*, vol. 108, no. 2, pp. 246–261, Feb. 2020.

[4] Z. Ren, Y. Huang, B. Du, and Y. Liu, "Reliable routing algorithm based on community for opportunistic networks," *J. Comput. Inf. Syst.*, vol. 10, no. 20, pp. 8873–8880, 2014.

[5] O. S. Oubbati, N. Chaib, A. Lakas, S. Bitam, and P. Lorenz, "U2RV: UAV-assisted reactive routing protocol for VANETs," *Int. J. Commun. Syst.*, vol. 33, no. 10, Jul. 2020, Art. no. e4104.

[6] I. Bor-Yaliniz and H. Yanikomeroglu, "The new frontier in RAN heterogeneity: Multi-tier drone-cells," *IEEE Commun. Mag.*, vol. 54, no. 11, pp. 48–55, Nov. 2016.

[7] N. Hossein Motlagh, T. Taleb, and O. Arouk, "Low-altitude unmanned aerial vehicles-based Internet of Things services: Comprehensive survey and future perspectives," *IEEE Internet Things J.*, vol. 3, no. 6, pp. 899–922, Dec. 2016.

[8] W. Shi, H. Zhou, J. Li, W. Xu, N. Zhang, and X. Shen, "Drone assisted vehicular networks: Architecture, challenges and opportunities," *IEEE Netw.*, vol. 32, no. 3, pp. 130–137, May 2018.

[9] O. S. Oubbati, A. Lakas, F. Zhou, M. Güneş, and M. B. Yagoubi, "A survey on position-based routing protocols for flying ad hoc networks (FANETs)," *Veh. Commun.*, vol. 10, pp. 29–56, Oct. 2017.

[10] N. Lin, L. Fu, L. Zhao, G. Min, A. Al-Dubai, and H. Gacanin, "A novel multimodal collaborative drone-assisted VANET networking model," *IEEE Trans. Wireless Commun.*, vol. 19, no. 7, pp. 4919–4933, Jul. 2020.

[11] P. Fondo-Ferreiro, F. Gil-Castiñeira, F. J. González-Castaño, D. Candal-Ventureira, J. Rodriguez, A. J. Morgado, and S. Mumtaz, "Efficient anchor point deployment for low latency connectivity in MEC-assisted C-V2X scenarios," *IEEE Trans. Veh. Technol.*, vol. 72, no. 12, pp. 16637–16649, Dec. 2023.

[12] S. Jobaer, Y. Zhang, M. A. I. Hussain, and F. Ahmed, "UAV-assisted hybrid scheme for urban road safety based on VANETs," *Electronics*, vol. 9, no. 9, p. 1499, Sep. 2020.

[13] H. Sedjelmaci, M. A. Messous, S. M. Senouci, and I. H. Brahmi, "Toward a lightweight and efficient UAV-aided VANET," *Trans. Emerg. Telecommun. Technol.*, vol. 30, no. 8, Aug. 2019, Art. no. e3520.

[14] M. Skocaj, N. Di Cicco, T. Zugno, M. Boban, J. Blumenstein, A. Prokes, T. Mikulasek, J. Vychodil, K. Mikhaylov, M. Tornatore, and V. Degli-Esposti, "Vehicle-to-everything (V2X) datasets for machine learning-based predictive quality of service," *IEEE Commun. Mag.*, vol. 61, no. 9, pp. 106–112, Sep. 2023.

[15] M. A. Khan, S. Ghosh, S. A. Busari, K. M. S. Huq, T. Dagiuklas, S. Mumtaz, M. Iqbal, and J. Rodriguez, "Robust, resilient and reliable architecture for V2X communications," *IEEE Trans. Intell. Transp. Syst.*, vol. 22, no. 7, pp. 4414–4430, Jul. 2021.

[16] V. Maglogiannis, D. Naudts, S. Hadiwardoyo, D. van den Akker, J. Marquez-Barja, and I. Moerman, "Experimental V2X evaluation for C-V2X and ITS-G5 technologies in a real-life highway environment," *IEEE Trans. Netw. Service Manage.*, vol. 19, no. 2, pp. 1521–1538, Jun. 2022.

[17] M. Z. Khan, M. A. Javed, H. Ghandorh, O. H. Alhazmi, and K. S. Aloufi, "NA-SMT: A network-assisted service message transmission protocol for reliable IoV communications," *IEEE Access*, vol. 9, pp. 149542–149551, 2021.

[18] Y. Zhou, N. Cheng, N. Lu, and X. S. Shen, "Multi-UAV-Aided networks: Aerial-ground cooperative vehicular networking architecture," *IEEE Veh. Technol. Mag.*, vol. 10, no. 4, pp. 36–44, Dec. 2015.

[19] O. S. Oubbati, A. Lakas, N. Lagraa, and M. B. Yagoubi, "CRUV: Connectivity-based traffic density aware routing using UAVs for VANets," in *Proc. Int. Conf. Connected Vehicles Expo. (ICCVE)*, Oct. 2015, pp. 68–73.

[20] X. Wang, L. Fu, Y. Zhang, X. Gan, and X. Wang, "VDNet: An infrastructure-less UAV-assisted sparse VANET system with vehicle location prediction," *Wireless Commun. Mobile Comput.*, vol. 16, no. 17, pp. 2991–3003, Dec. 2016.

[21] O. Chughtai, M. Naeem, and K. A. Khaliq, "UAV-assisted cooperative routing scheme for dense Vehicular ad hoc network," in *Intelligent Unmanned Air Vehicles Communications for Public Safety Networks*. Cham, Switzerland: Springer, 2022, pp. 199–214.

[22] Q. Usman, O. Chughtai, N. Nawaz, Z. Kaleem, K. A. Khaliq, and L. D. Nguyen, "A reliable link-adaptive position-based routing protocol for flying ad hoc network," *Mobile Netw. Appl.*, vol. 26, no. 4, pp. 1801–1820, Aug. 2021.

[23] M. Li, Z. Li, S. Wang, and S. Zheng, "Enhancing cooperation of vehicle merging control in heavy traffic using communication-based soft actor-critic algorithm," *IEEE Trans. Intell. Transp. Syst.*, vol. 24, no. 6, pp. 6491–6506, Jun. 2023.

[24] O. Kavas-Torris, S. Y. Gelbal, M. R. Cantas, B. A. Guvenc, and L. Guvenc, "V2X communication between connected and automated vehicles (CAVs) and unmanned aerial vehicles (UAVs)," *Sensors*, vol. 22, no. 22, p. 8941, Nov. 2022.

OMER CHUGHTAI (Member, IEEE) received the B.Eng. degree in computer science with a focus on IT from the University of Engineering and Technology, Taxila, Pakistan, the M.S. degree from COMSATS University Islamabad, Wah Campus, Pakistan, and the Ph.D. degree from Universiti Teknologi PETRONAS, Malaysia. In addition to his academic pursuits, he has a varied professional background, having held roles in the industry. He is currently a tenured Associate Professor with the Department of Electrical and Computer Engineering, COMSATS University Islamabad. He is an experienced professional in computer science and engineering with more than 20 years of expertise. He has a strong publication history, an impressive record of securing research grants, and holds two patents. His achievements have not only gained him recognition but also reflect his dedication to mentoring Ph.D. and M.S. students. His research interests include cross-layer protocol design, routing in low-power wireless ad hoc networks, traffic load balancing, the IoT networks, artificial intelligence, vehicular and flying ad hoc networks, and mobility and resource management in heterogeneous networks. He is an active member of esteemed organizations, such as the Internet Society (ISOC), where he was honored with an Internet Engineering Task Force (IETF) Fellowship. He is also a valued member of the Wireless Networks Laboratory (WiNeT Lab), contributing to state-of-the-art technologies. His honors include the Research Productivity Award and a Letter of Appreciation. He was awarded a fully-funded Ph.D. Research Scholarship from Universiti Teknologi PETRONAS.

NADIA NAWAZ QADRI (Senior Member, IEEE) received the B.E. degree in computer systems engineering and the M.E. degree in communication systems and networks from the Mehran University of Engineering and Technology, Jamshoro, Pakistan, in December 2002 and December 2004, respectively, and the Ph.D. degree in electronic systems engineering in electronic systems engineering, in June 2010. From 2003 to 2004, she was a Laboratory Lecturer with the Mehran University of Engineering and Technology. From 2004 to 2005, she was a Lecturer with Fatima Jinnah Women University, Rawalpindi. In October 2005, she joined the COMSATS Institute of Information Technology (CIIT), Wah Campus. From CIIT, she proceeded to U.K. for the Ph.D. degree funded by CIIT, under HEC's "Faculty Development Program," in 2006. Then, she joined the Department of Electrical and Computer Engineering, COMSATS University Islamabad (CUI), Wah Campus, as an Assistant Professor, where she is currently a Professor and a Research Focal Person (ORIC). She has more than 20 years of teaching and research experience at renowned universities of Pakistan. Her research interests include video streaming, mobile ad hoc networks and vehicular ad hoc networks, P2P networks, wireless sensor networks, video and image processing, 4G and 5G communication, smart grids, the Internet of Things, and multicore reconfigurable architectures.

ZEESHAN KALEEM (Senior Member, IEEE) is currently an Associate Professor with COMSATS University Islamabad, Wah Campus. He has published more than 100 technical papers and patents. He served as a TPC Member for world-distinguished conferences, such as IEEE Globecom, IEEE VTC, IEEE ICC, and IEEE PIMRC. He consecutively received the National Research Productivity Award (RPA) Awards from the Pakistan Council of Science and Technology (PSCT), in 2017 and 2018, and the Higher Education Commission (HEC) Best Innovator Award, in 2017, and there was a single award all over Pakistan. He was also a recipient of the 2021 Top Reviewer Recognition Award for IEEE TRANSACTIONS ON VEHICULAR TECHNOLOGY. He is currently serving as a Technical Editor for several prestigious journals/magazines, such as IEEE TRANSACTIONS ON VEHICULAR TECHNOLOGY, *Computer and Electrical Engineering* (Elsevier), *Human-centric Computing and Information Sciences* (Springer), *Journal of Information Processing Systems*, and *Frontiers in Communications and Networks*, and the Track Chair of "Recent Results" at IEEE VTC2024-Spring, Singapore. He has served/serving as a Guest Editor for Special Issues in IEEE WIRELESS COMMUNICATIONS, *IEEE Communications Magazine*, IEEE ACCESS, *Sensors*, IEEE/KICS JOURNAL OF COMMUNICATIONS AND NETWORKS, and *Physical Communications*.

CHAU YUEN (Fellow, IEEE) received the B.Eng. and Ph.D. degrees from Nanyang Technological University (NTU), Singapore, in 2000 and 2004, respectively. He received the IEEE Asia Pacific Outstanding Young Researcher Award, in 2012, and the IEEE VTS Singapore Chapter Outstanding Service Award, in 2019. He serves as an Editor for the IEEE TRANSACTIONS ON VEHICULAR TECHNOLOGY, IEEE SYSTEM JOURNAL, and IEEE TRANSACTIONS ON NETWORK SCIENCE AND ENGINEERING. He is a Distinguished Lecturer of the IEEE Vehicular Technology Society.